Proceedings of OMAE'02
21st International Conference on Offshore Mechanics and Arctic Engineering
June 23-28, 2002,Oslo, Norway

OMAE2002-28307

CHALLENGES IN THE DESIGN OF AN OFFSHORE WIND TURBINE FOUNDATION FOR ARCTIC CONDITIONS

Alistair E. Gill BEng AMIMechE,
Consultant to Advanced Engineering Services,
AMEC, City Gate, Aberdeen, Scotland.
Tel: +44 (0)1224 291 505
e-mail: alistair.gill@amec.com

Dr Ramsay Fraser FIStrucE, AMEC Advanced Engineering Services
City Gate, Aberdeen, Scotland.
Tel: +44 (0)1224 291 072 e-mail:
ramsay.fraser@amec.com

ABSTRACT

NEG Micon's Yttre Stengrund Offshore Wind Turbines in the Kalmarsund, Sweden, are supported on unique foundations designed by AMEC. The chosen foundation comprised a steel monopile secured into a rock socket drilled out beneath a deep layer of overlying soil. Sea-ice loading and fatigue governed the design. To minimise the sea-ice loads the foundation was fitted with an ice protection shield. In order to achieve the required fatigue life, time domain simulations were conducted to determine the response of the turbine to combined wind and wave action. Details of the fatigue analyses and methods used to calculate the sea-ice loading are presented herein.

INTRODUCTION

NEG Micon A/S has recently commissioned an offshore wind farm at Yttre Stengrund, (YS), in the Baltic Sea, off the Southeast coast of Sweden. The wind farm consists of five 2MW NM72 wind turbines. The turbines are located approximately 5Km offshore in between 6.8m and 8.6m of water. Figure 1 shows the geographical location of the wind farm.

NEG Micon awarded a contract for the design of the foundation structure with AMEC. Under the terms of the contract AMEC assumed full responsibility for undertaking the design, construction and installation of suitable foundation structures. AMEC's Advanced Engineering Services department, (AES), undertook the design. A further condition of the contract was that an independent certification of the foundation design by Det Norske Veritas (DNV) be obtained.

The local geology and sub-arctic environment at the site, coupled to the technical specification and tight development timetable, created a number of challenges. This paper aims to describe some of the technical difficulties encountered during the development of the foundation and how they were overcome.

NOMENCLATURE

M_x = the moment about the x-axis (Nm)
M_y = the moment about the y-axis (Nm)
F_z = the vertical force (N)
I = the second moment of area of the monopile (m^4)
r = the outer radius and A is the section area (m)
b = the width of the structure (m)
σ_{ip} = the compressive strength of ice (Pa)
σ_t = flexural strength of ice (Pa)
h = thickness of ice (m)
k_1 = a shape factor = 0.9 for cylinders
k_2 = the ice to structure contact factor = 1.0
k_3 = shape ratio factor = $\sqrt{(1+5(h/b))}$
ρ_w = density of water (kg/m^3)
g = acceleration due to gravity = $9.81 m/s^2$
$F_{H\ cone}$ = horizontal force against ice cone (N)
$F_{V\ cone}$ = vertical force against ice cone (N)

D = diameter of the ice cone at waterline (m)
D_T = diameter at the top of the ice cone (m)

α = cone angle from horizontal (deg)
μ = coefficient of friction
A_1-A_4 = coefficients, as functions of ρ_w, g, σ_t, h, α and μ
B_1-B_2 = coefficients, as functions of α and μ
L = the characteristic length of the floe (m)
C & D = buckling coefficients
R = truncated distance from the wedge apex to L (m)
B = width of beam at R (m)
γ_w = unit weight of water (N/m^3)
E = Elastic modulus of ice (Pa)
ν = Poisson's ratio of ice
l = is a shape factor
f_c = is a contact factor
V = the floe velocity (m/s)

GEOTECHNICAL DESCRIPTION OF THE SITE

The seabed at Yttre Stengrund comprised a layer of Quaternary glacial till of between 8.4m and 12.6m depth above sandstone bedrock. The soil was classified as a sandy and gravely till having a variable boulder and cobble content. Boulders of both Cambrian sandstone and Precambrian granite were present. The sandstone bedrock was quartzitic containing some mudstone and siltstone laminations. Weathering was limited to the upper most layers. Mechanical properties of both the soil and rock were determined through a Site Investigation, (SI), and laboratory testing managed by NEG Micon. Further details of the geotechnical properties are confidential.

METOCEAN DATA

NEG Micon provided a description of the wind climate at the site. Model data was supplemented by on site measurements collected by NEG Micon. The predicted annual 1 hour mean wind speed for the site was 8.25m/s, however for design purposes a slightly higher value was assumed for all load calculations. The key data are summarised in Table 1.

Table 1 YS Design Wind Climate

Annual 1 hr mean wind velocity	8.5 m/s
50 yr extreme 2sec gust velocity	50 m/s
Air density	1.28 Kg/m
Turbulence intensity	13%

A wave study was carried out by Sveriges Meteorologiska och Hydrologiska Institut (SMHI) using the Simulating Waves Nearshore (SWAN) model, [**1**], in conjunction with 21 years of wind and wave measurements at Öland Södra Grund (OSG) lighthouse. The model was run with a coarse grid to model the larger area south of the Kalmarsund and a fine grid for the area close to the YS site. A total of 176 SWAN simulations were run comprising 11 wind speed bins of eight directions for each grid. This enabled SMHI to provide Sea-state spectra for each heading as a function of wind speed. This proved particularly useful for the fatigue analysis. The wave climate at YS is summarised in Table 2.

Table 2 YS Oceanographic Data

Water depth	7.7 m to 8.6m
H_s (50 yr return)	4.5m
T_z (50 yr return)	8.5s
H_{max} (50 yr return)	7.64m
T_{ass} (50 yr return)	12s
Max mean sea level variation	+1.2m/ - 0.9m
Storm wind induced current	0.5m/s
Tides and seiches	negligible
Sea water density	1010 kg/m^3

SEA ICE DATA

The Kalmarsund can become frozen during the winter months. In severe winters the YS site is affected by consolidated drift ice. The last severe winter was 1987. The area surrounding YS is affected by a variety of ice conditions. These are summarised in Table 3.

Table 3 YS Sea Ice Conditions

Thickness (mm)	Floe Size (m)	Floe Velocity (m/s)
<100	1000+	0.5
300	1000	0.25
400	100	0.25
1000	30	0.25

The compressive strength of the ice is based on measurements taken from warm porous ice in the Gulf of Bothnia. To the authors' knowledge the flexural strength of the ice at YS has never been measured. Therefore the flexural strength was based on tests conducted on fresh water ice. In both cases the values agreed with those obtained by DNV. The only data available describing ice conditions at YS is included in Table 4.

Table 4 Ice Formation

Occurrence Probability (%)	Date of Formation	
	Ice >0cm Thick	Ice > 15cm Thick
3-20	19 Dec – 12 Jan/ 26 Mar – 20 April	8 Jan – 10 Feb/ 15 Mar – 8 April
20-30	13 Jan – 2 Feb/ 3 Mar – 25 Mar	11 Feb – 14 Mar
30-40	3 Feb – 16 Feb/ 15 Mar – 19 Mar	-
40-50	17 Feb – 14 Mar	-

CHOSEN FOUNDATION CONFIGURATION

The seabed would have been suitable for various foundation types, such as monopile, gravity base or tripod. However, due to the tight project timescale NEG Micon decided early in the development that there was insufficient time to develop gravity or tripod solutions. Therefore they specified that the foundation be a monopile. The challenge for AMEC was to make a monopile solution work.

The depth of soil alone did not provide sufficient lateral support for a monopile design (a depth of approximately 20m would have been required). Therefore the foundation had to penetrate significantly into the bedrock. The strength of the rock excluded a driven pile solution and meant that a socket had to be drilled into the rock to secure the base of the pile. The need to drill out a rock socket beneath the glacial till led the design team to consider two options:

i. A spigot grouted through the monopile into the rock socket. The monopile would be inserted first by drilling and surging down to rock level. Then it would and act as its own cofferdam while the rock socket was drilled.
ii. A monopile grouted directly into a rock socket drilled out through a separate casing. Figure 2 shows the two configurations.

Both options would have enabled a single drill diameter to be used, which was an important cost consideration. However, option i) provided easy means of correcting any vertical misalignment of the foundation, (a specified requirement) and placed more reliance on the strength of the grout joint. Option ii) was selected.

A Finite Element (FE) solid model of the entire foundation was generated in ABAQUS. This was used to determine the stresses within the monopile, grout and rock socket. The FE model comprised ABAQUS Axisymmetric-Asymmetric solid elements. This ABAQUS element was chosen as it permitted non-symmetric loading, modelled pile ovality under load and remained computationally economical. Figure 3 shows the layout of the model.

The soil and rock were modelled as an elastic continuum with mechanical properties extracted from the SI report. The solid model was validated against a beam element FE model in which the soil was represented by non-linear p-y springs and the rock by an elastic stiffness.

The solid model proved invaluable, as it enabled a number of areas of interest to be examined within a single model, those being:

i. Top flange weld detail Stress Concentration Factor (SCF)
ii. Transition cone weld SCF
iii. Monopile, rock socket & grout stress distributions
iv. Combined soil and rock behaviour.

The output from i), ii) and iii) were used as inputs to the fatigue analysis. They identified areas of high stress concentration, notably the top flange and transition cone where more detailed models were developed from which more accurate SCFs were derived.

The model accounted in full for the interaction between the pile, the grout, the casing and soil down the length of the foundation. The stresses in the pile and grout at the critical positions of the casing top and at rock level were then used to determine the pile strength interaction ratios in accordance with API, [2]. The stress levels in the grout highlighted the potential for shear and tensile failure of the grout and grout/steel interface. This was accounted for by including slip planes in the model between the steel, grout and rock. By modelling the slip planes the structural integrity of all components of the foundation could be guaranteed regardless of the condition of the grout over time.

The foundation configuration proved generally insensitive to the range of soil properties encountered.

FATIGUE LIFE

Cyclic loading of the foundation was generated by a combination of aerodynamic and hydrodynamic loading. To accurately predict this loading a series of time domain simulations of the combined wind and wave environment was conducted using the BLADED, [3]. NEG Micon provided the initial aeroelastic BLADED model of the wind turbine. This model was then modified for the offshore environment by AES. The conversion of the model to the offshore environment included:

i. the foundation geometry of a number of different pile dimensions
ii. the addition of wave and other hydrodynamic parameters
iii. the position of the foundation fixity depth to account for the variation in water depth across the site.

The key advantage of this approach was that it accounted fully for the combined effects of the aerodynamic and hydrodynamic loading making the prediction of the stress history of the structure as realistic as possible. The economic disadvantages of using a time domain approach are becoming much less pronounced with the latest generation of computing hardware, particularly when compared to the cost of an excessively conservative foundation design.

Previous offshore wind farm foundation designs carried out by AES addressed the hydrodynamic and aerodynamic loading separately. Determining the aerodynamic and hydrodynamic fatigue damage individually and then combining them using a sum of the root of the squares approach (or similar) is perfectly valid and usually leads to a conservative design. However, to keep the degree of conservatism down more advanced methods were employed here.

The time domain simulations were used to generate a rainflow count of the stress ranges within the pile. The procedure adopted for this was as follows:

Wind speed bands from 0-3m/s to 35-40m/s were allocated for each wind/wave approach direction. In total 90 load cases were generated, each representing a different speed or direction. Turbine operation was modeled between the start up and cut out velocities, 3m/s to 25m/s. Outside these limits the turbine was considered to be at a standstill, or "Parked".

A 3D turbulent wind volume was generated within BLADED for each mean wind speed band and stored on file. The height and width of the volumes were set to encompass the full swept area of the rotor and tower and the length set according to the mean wind speed and length of simulation required. Turbulence was super-imposed on the mean wind speed values based on the turbulence intensity.

The sea state spectrum associated with each mean wind speed band was input to the model. A random sea-state was then simulated in BLADED for each spectrum and stepped past the foundation. Each simulation was 20 minutes in duration with a different random number seed used in the realization of each sea-state. In parallel to this, BLADED stepped the 3D turbulent wind model past the rotor and tower at the mean wind speed.

The persistence, P, for each wind speed band was derived from the wind heading, based on a wind rose supplied by NEG Micon and sea-state heading distributions supplied by SMHI. The wind speed was assumed to be Weibull distributed with Weibull parameter k=2. P was therefore calculated by taking the product of the wind speed probability and the wind/sea heading probability as percentages of total time.

A rainflow count of the stress range in the foundation was determined from the stress history derived from the simulations. The fatigue lives of the critical structural elements were then calculated from that rainflow count. The rainflow count was initially calculated assuming uni-directional loading; i.e. all loading was lumped from a single direction. This proved to be too onerous an assumption without significantly increasing the pile weight. Therefore additional analysis was carried out to account for the directional nature of the loading and hence fatigue damage.

GENERATING A DIRECTIONAL RAINFLOW COUNT

The stress at any position, O, around the circumference of the monopile varied with wind direction, see Figure 4. To account for this variation the stress history for each position was developed from the load time histories of each force component. The axial stress, σ_o, at point O, was expressed as a function of the wind/wave direction, θ, and the individual aerodynamic and hydrodynamic force components, M_x, M_y and F_z, as per Eq 1.

$$\sigma_o = \frac{M_y}{I} \times r \times \sin\theta - \frac{M_x}{I} \times r \times \cos\theta + \frac{F_z}{A} \qquad (1)$$

As the wind/wave direction changed, the axial stress at that fixed position also changed. An axial stress history was generated from the individual force component histories for eight positions A to H around the pile for all wind and wave cases. Each force component history, for M_x, M_y etc was factored and then combined into a stress signal using Eq 1. Only M_x, M_y and F_z needed to be considered because only these forces contributed to the stresses in the pile wall that cause fatigue damage. A stress signal, σ_1, defined as the total stress history at position A was derived by combining the stress histories at A, σ_A, from eight wind/wave headings (0^o, 45^o …315^o) giving:

$$\sigma_1 = \sum_{i=1}^{8} \sigma_{A}^{\text{for } i^{th} \text{ wind direction}} \qquad (2)$$

Stress signal, σ_2, was the total stress history at position B and so on, until 8 stress signals were developed. The rainflow count of stress range at each location was then calculated from these signals.

The fatigue damage was calculated from the rainflow count using a spreadsheet to perform the calculations. This made it easier to iterate the choice of structural detail to maximize fatigue life, without having to reprocess the stress signals each time the structural detail was altered. Figure 5 summarizes the above procedure.

This optimized the pile dimensions, making a saving in steel of over 20 tonnes per pile while maximizing the achieved fatigue life. However, a number of the structural details hampered attempts to achieve the required fatigue life. Two of these proved particularly troublesome, namely the J-tube penetrations and the transition cone. The former will be described in more detail.

J-TUBE PENETRATIONS

The client had specified that they required an internal cable duct, or J-tube, penetrating the pile just above seabed. This was an attempt on their part to minimize sea ice loading on the cable ducts and to ease cable installation. However, the necessity to house the cable duct inside the pile at such a low elevation created inherent fatigue problems, as the bending stresses in the pile are higher. This initially prevented the required fatigue life from being achieved. However, by demonstrating that the fatigue damage was directional and quantifying the degree of directionality, it was possible to locate the J-tube penetrations at the points on the pile circumference of least damage. In addition, care was also taken in the detail design of the penetration itself to maximize the fatigue life.

A finite element shell model of the penetration was created using ABAQUS. This was used to compare stress concentration factors at each position within the penetration and to optimize the detail design of the penetration itself. The final configuration of the J-tube penetration optimized the

combination of stress concentration factor and weld detail to maximize the fatigue life.

FLEX 5 ANALYSIS

NEG Micon conducted an independent combined wind and wave time domain analysis using the FLEX5 programme in parallel to the foundation design. This gave results consistent with those from BLADED.

SEA ICE LOADING

The second major challenge for the foundation design was dynamic sea ice loading. Not only was there an engineering necessity to ensure the foundation could withstand the loads involved, there was also the requirement to convince the certifying authority that this was the case. The latter proved just as challenging as the engineering.

The sea ice loads on a wind turbine foundation depend on many factors including:

i. Ice mechanical properties, e.g. strength & ductility
ii. Ice thickness
iii. Floe size, concentration and movement
iv. Structure shape.

Of these the first three are site-dependent. The ice thickness, floe concentration and coverage depend upon the temperature, the strength of the wind and the prevailing sea state conditions. Temperature, salinity and strain rate also influence the mechanical properties of the ice. The ice conditions have a direct role in determining the loads on the structure. How they are interpreted can significantly alter the design premise and as a consequence the effort required for certification by a third party. Of all of the factors involved, the design team can only influence the shape of the foundation.

Setting aside the mechanical properties of the ice and its thickness, the ice load can be static or dynamic depending upon the speed the ice moves. The guidance that is available offers the designer only two design conditions:

i. Static ice loading
ii. Dynamic ice loading

For static ice loads a number of well established formulae exist for the load on a vertical or inclined structure. Here they are taken from reference [4].
For a vertical structure:

$$F_{vert} = k_1 k_2 k_3 b h \sigma_{ip} \tag{3}$$

For an upward sloping structure, (related formulae exist for a downward sloping structure):

$$F_{H_{cone}} = \left[A_1 \sigma_t h^2 + A_2 \rho_w g h D^2 + A_3 \rho_w g h \left(D^2 - D_T^2\right)\right] A_4 \tag{4}$$

$$F_{V_{cone}} = B_1 H + B_2 \rho_w g h \left(D^2 - D_T^2\right) \tag{5}$$

These were used to calculate the static ice loads on the monopile.

For dynamic loading, a lesser force magnitude was assumed, reference [5]. This was applied to the structure as a sinusoidal load at the natural frequency. The dynamic response to the sinusoidal load over-utilized the pile once the ice thickness was greater than 100mm. Because the ice could reach 300mm in thickness, ways of limiting the dynamic ice load had to be found.

SEA ICE LOADS LIMITED BY PROBABILITY

The probability of consolidated ice affecting the site was 20-30%. This was too high to discount dynamic ice loading on the basis of the likelihood of occurrence.

SEA LOADS LIMITED BY DRIVING FORCE

The wind and wind-generated current comprise the dominant driving force of the floes in the Kalmarsund. The driving force acting on the floe is a function of the floe surface area and its surface roughness. However, there is some uncertainty in ice surface roughness and the possibility of additional loading through the ice pack existed. Therefore it was concluded that the driving force would not limit the ice load.

LOADS LIMITED BY ICE STRENGTH

A. BUCKLING

The buckling load, P, of a wedge of ice was checked using the following approximation, [6].

$$\frac{P}{B \cdot \gamma_w \cdot L^2} = C + \frac{D}{R/L} \tag{6}$$

with

$$L = \left[\frac{E \cdot t^3}{12 \cdot \gamma_w \cdot (1-\nu)^2}\right]^{1/4} \tag{7}$$

This showed that for a 1000m long wedge the buckling loads were well in excess of the crushing limit, for even the thinnest ice.

B. SPLITTING

The potential for splitting the ice floe by altering the shape of the pile at the water line was considered. The Korzhavin equation, [6], for calculating ice pressure on bridge piers, was considered:

$$p_e = \frac{2.5 \cdot l \cdot f_c}{V^{1/3}} \cdot \sigma_{ip} \tag{8}$$

However, this did not reduce the ice pressure significantly for the floe velocities of interest. The reliability of a floe splitting device was also questioned, and discounted on the following grounds:

i. Floe splitting is governed by ice fracture toughness and no data was available for Baltic ice.
ii. Consolidated drift ice may behave differently from single floe pieces as consolidation pressure affects how a floe splits. No published data could be found to support such a device without having experimental evidence to confirm performance.

C. BENDING

Research by Karna, [7], and others suggests that the response of slender structures to ice loading is largely governed by the speed of the floe rather than directly by the thickness of the ice sheet, (as would be the case for the static ice condition). The thickness of the ice plays an important role in limiting the response of the structure, but it does so by restricting the velocity at which dynamic interaction can occur. This research indicates that there is an upper bound and lower bound velocity outside of which the dynamic response of the structure drops off dramatically. This has important implications for offshore wind turbine design in arctic conditions as it offers the potential to limit the load.

However, this research was not accepted by DNV as sufficient justification to limit the ice thickness that should be considered in the dynamic ice-loading scenario. So any potential relationship between the floe speed, ice thickness and dynamic ice interaction was not used in this instance.

The data available for Yttre Stengrund suggested there were two scenarios in which dynamic ice loading was likely. First, during the earlier part of the winter thin ice (<10cm) drifts South along the coast, at floe velocities of up to 1knot (0.5m/s). Second, in the spring the consolidated ice sheet begins to melt and break up. Here the ice thickness could conceivably be up to the maximum consolidated sheet thickness of 300mm. In this scenario the floe velocity is typically less than 0.5 knots (0.25m/s).

Because of the possibility that thick ice could cause dynamic loading the pile was fitted with a conical ice shield. This had two beneficial effects. First, it reduced the static ice loads and second, it would act to prevent, or at least delay, the lock-on interaction between the ice sheet and the structure that triggers resonant loading. This is because the failure mechanism within the ice changes from continuous crushing to discontinuous bending. The change from crushing to bending reduced the total load because the flexural strength of the ice was significantly lower than the crush strength. The failure of the ice by flexure also increases the breaking length of the ice. Therefore the ice sheet would have to travel further before it re-established contact with the structure and begin a new load cycle. It must therefore travel faster to couple the load cycle with the natural frequency of the structure. Although vibrations would still be possible with the ice cone fitted, the floe velocity required to excite the natural frequency would be greatly increased.

Because there was a limit to the floe velocities found at Yttre Stengrund, the thickness of ice that must be considered for dynamic loading could also be limited. The maximum velocity of the consolidated ice sheet seen at Yttre Stengrund was around 0.5 knots, (0.25m/s). SMHI recommended a breaking length of the ice, L_B, of 1/3 of the characteristic floe length, L. This would result in a breaking length of 1.5m for a 300mm thick floe. The ice would need to travel 1.5m during the natural period of the tower for the ice loading to couple with the natural frequency. So the velocity of the ice to cause "lock-on" was approximated by:

$$\frac{L_B}{V} = \frac{1}{\lambda} \tag{9}$$

It is important to realize that this assumes that the breaking length is constant. The floe composition may have an influence on this and the breaking length could vary as refrozen cracks or leads interfere with the breaking process. However, this would reduce the likelihood of resonance as the load/structure interaction would be disrupted further. In such circumstances the loading frequency would be more random than harmonic.

Given that the floe velocity could be limited to 0.25m/s for the thickest ice, we could discount dynamic ice loading with 0.3m ice for Yttre Stengrund, provided an ice cone was fitted, as the floe velocity would not be sufficient to couple the ice with the structure.

The breaking length is also a function of ice thickness, some research suggests $L_B \approx 7h$, [8]. In any event, it is likely to be less with thinner ice, so there could still be dynamic loading, albeit with thinner ice, with the floe velocities seen at Yttre Stengrund. The upper bound ice thickness used for dynamic loading was therefore found by keeping the ratio of the breaking length to ice thickness constant, L/3. This limited the ice thickness to 128mm.

Having established an upper bound ice thickness for dynamic ice loading with the cone fitted, the structural response to dynamic ice forces with and without an ice cone were compared using a FE beam model of the entire structure. The load was assumed to be harmonic and 1.5% of critical damping was applied. This represents the case where the turbine blades are parked at wind speeds above 25m/s. The degree of damping is higher when the turbine is in operation.

Figure 6 shows a comparison between the response of the structure with and without an ice cone. The relative moments at the mudline are shown for a range of loading frequencies. The dynamic response peak corresponds to loading applied at the natural frequency. The moments have been normalized with respect to the maximum response. The reduction in loading with the ice cone is substantial. Other considerations accounted for in the design of the ice protection cone included:

i. Additional hydrodynamic load
ii. Water level variation

iii. Local strength of the ice cone
iv. Method of attachment to the pile

ADDITIONAL LOADING

The presence of the ice cone increased the hydrodynamic loads. However, judicious dimensioning of the cone kept this increase to a minimum. A double-sided cone was chosen to accommodate the variation in water level while keeping the total diameter of the cone and the increase in the hydrodynamic load to a minimum.

The presence of the ice cone resulted in an increase of 14% in the storm wave loading at the deepest water location. The external shape of the ice cone was included in the BLADED fatigue model so that the additional hydrodynamic load was also accounted for in the fatigue analysis.

ICE CONE STRENGTH AND PILE FATIGUE

The ice protection cone added to the local stiffness of the monopile. Consequently, its presence changed the stresses in the monopile and so this had to be accounted for in the fatigue analysis. Additionally, the cone and its attachment mechanism had to be robust enough to withstand the ice pressure and wave loading.

A FE model of the ice protection shield was created to examine the stresses both within the ice cone itself and within the pile wall. The FE analysis confirmed that the local strength of the cone was sufficient to withstand the ice pressure and wave loading while also providing SCFs at the connection between the cone and the pile. Figure 7 shows one of the models used.

It was decided to weld the ice cone directly to the monopile to ensure adequate strength and minimise potential maintenance. However, the fabrication sequence of the cone and pile was adjusted to ensure the weld detail was of an adequate fatigue classification.

CONSEQUENCES OF INCLUDING THE ICE CONE

The necessity to equip the pile with an ice cone to minimize the risk both to the structural integrity of the foundation and of it receiving DNV certification did not come without a number of significant implications. The ice cones made a significant contribution to the unit costs of the monopiles. The transportation and handling of the piles during installation were all made more difficult with the ice cones present.

CONCLUDING REMARKS

Yttre Stengrund provided AMEC's design team with the opportunity to consolidate its offshore wind turbine track record. It provided a number of challenges, notably marrying the physical configuration required by the client with the need for a long fatigue life and countering the potential for dynamic sea-ice loading.

ACKNOWLEDGEMENTS

The authors would like to thank their colleagues at NEG Micon for permission to publish this paper and for providing the BLADED software and turbine model.

Particular thanks go to Peter Fish of NEG Micon UK Offshore Technology Group who managed the design work from the NEG Micon side and prepared the technical specification, geotechnical and metocean data and who also helped review this paper. Dick Veldkamp also of NEG Micon, carried out the independent analysis using FLEX5. Both Peter and Dick are thanked for their valuable technical input.

REFERENCES

1. Booij, Ris and Holthuijsen, 1999, A third-generation wave model for coastal regions, 1. Model description and validation. Journal of Geophysical Research Vol. 104, No C4.
2. API RP 2A- LFRD, 1st Ed, 1993, Recommended Practise for Planning, Designing and Constructing Fixed Offshore Platforms – Load and Resistance factor design.
3. Garrad Hassan, June 1999, BLADED for Windows, Version 3.38.
4. XIth Conference Of the International Association of Light House Authorities. 1985. Final Report of the IALA Technical Committee to Study the Effect of Ice on Lighthouse Structures. Chaired by Prof. Mauri Määtänen.
5. Haapanen, Määttänen & Koskinen, Offshore Wind Turbine Foundations in Ice Infested Waters, Helsinki University.
6. API RP2N 2nd Ed, 1995, Recommended Practise for Planning, Designing and Constructing Structures and Pipelines for Arctic Conditions
7. Kärnä, 1993, Steady-state Vibrations of Offshore Structures, 1st Conference on the Development of the Russian Arctic Offshore.
8. Yue, Q., Bi, X., Yu, X., 2000, Effect of Ice-breaking Cones for Mitigating Ice-Induced Vibrations, IUTAM Symposium "Scaling Laws in Ice Mechanics and Ice Dynamics", Fairbanks,AK, USA.

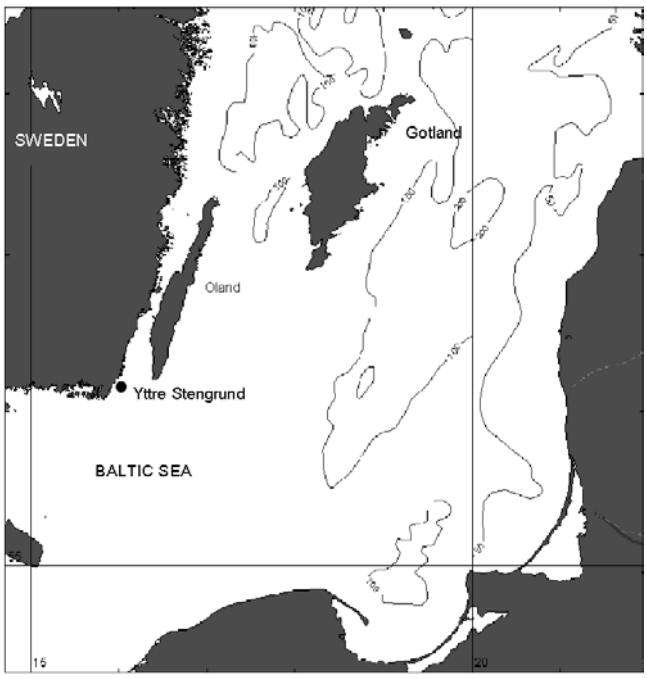

Figure 1: Yttre Stengrund Location

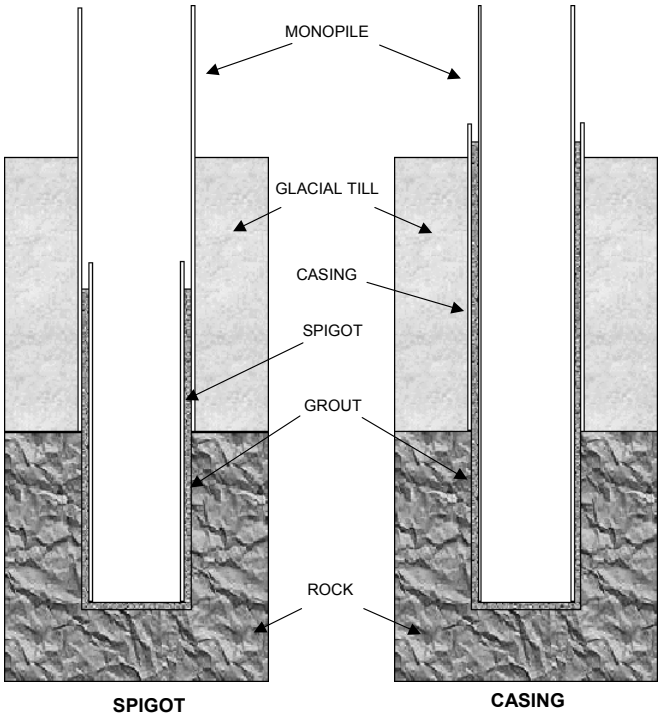

Figure 2: Monopile Concepts Evaluated

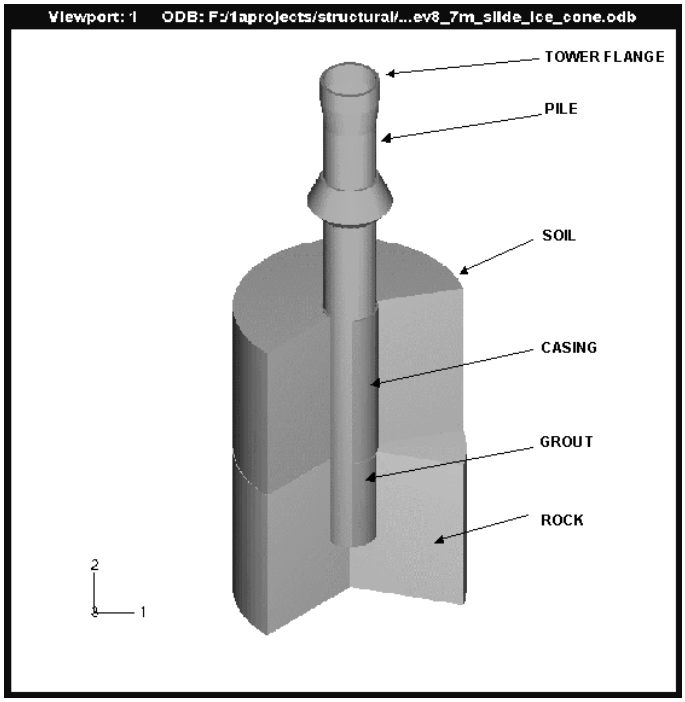

Figure 3: ABAQUS Solid FE Model of Foundation

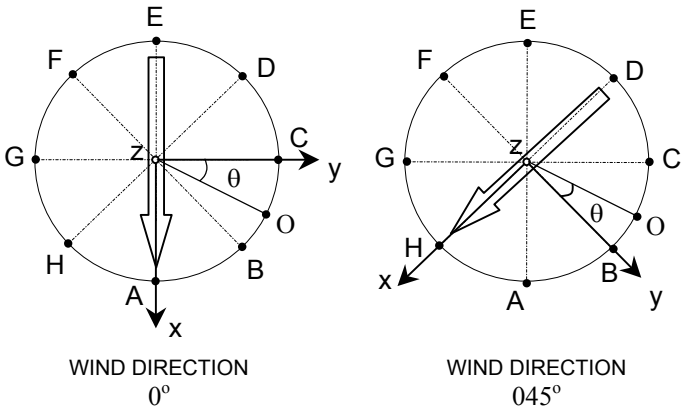

Figure 4: Stress Distribution Around Monopile

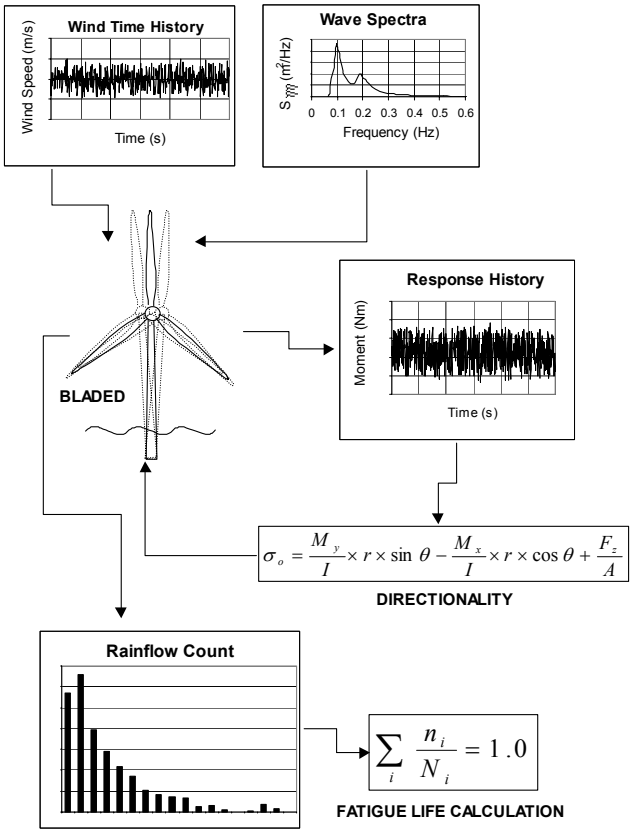

Figure 5: Summary of Fatigue Assessment Procedure

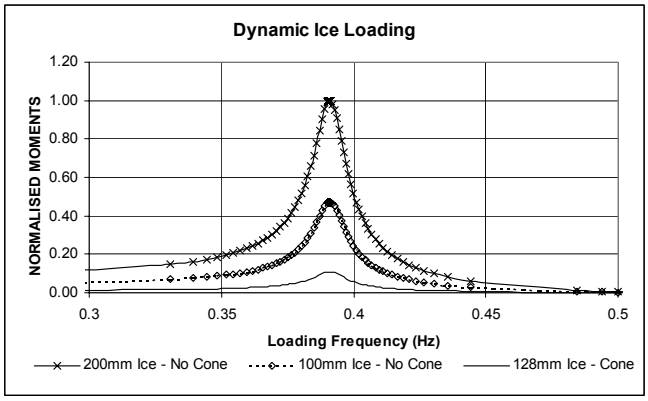

Figure 6: Dynamic Response to Sea Ice Loading

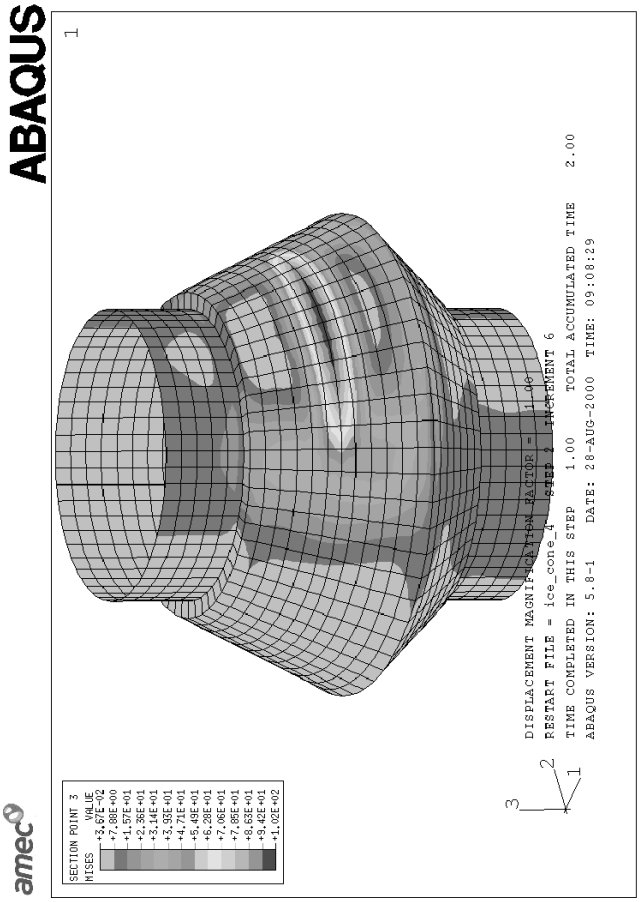

Figure 7: Finite Element Model of Ice Cone